

Learning Human Perspective in Line Drawings from Single Sketches

JINFAN YANG, University of British Columbia, Canada
 LEO FOORD-KELCEY, University of British Columbia, Canada
 SUZURAN TAKIKAWA, University of British Columbia, Canada
 NICHOLAS VINING, NVIDIA, University of British Columbia, Canada
 NILOY MITRA, University College London, United Kingdom
 ALLA SHEFFER, University of British Columbia, Canada

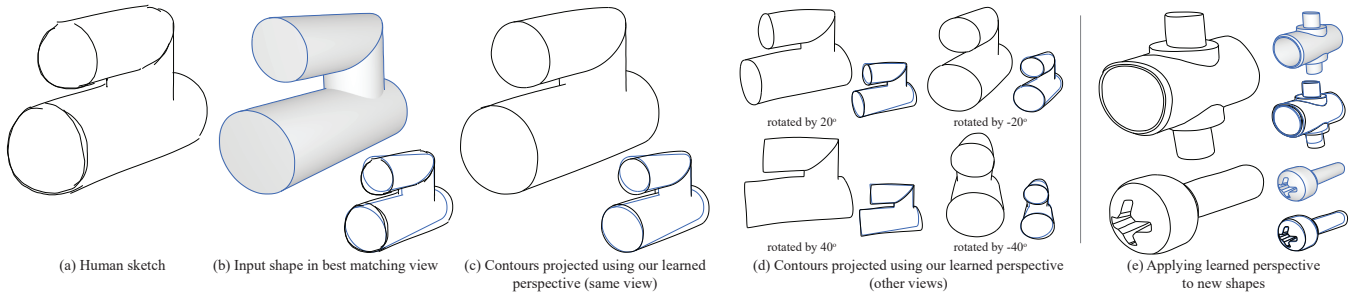


Fig. 1. Human sketches (a) use a perspective projection that deviates from the standard analytical perspective model (b). The *deviation* between artist’s and best approximating analytic perspective (b) is highlighted in the inset (human sketch in black, analytically projected contours in blue). Given the 3D object depicted in the sketch (b), we model and learn the *human perspective* (c). We apply the learned perspective to render the object from nearby views (d) and transfer it to similar shapes (e). Insets show analytically projected contours overlaid with human sketch (b) or contours projected using our perspective (c,d). For example, note how circular faces appear elliptical under analytic perspective but are sketched to be more circular in human and our outputs.

Artist-drawn sketches only loosely conform to analytical models of perspective projection. This deviation of human-drawn perspective from analytical perspective models is persistent and well known, but has yet to be algorithmically replicated or even well understood. Capturing *human perspective* can benefit many computer graphics applications, including sketch-based modeling and non-photorealistic rendering. We propose the first dedicated method for learning and replicating human perspective. A core challenge in learning this perspective is the lack of suitable large-scale data, as well as the heterogeneity of human drawing choices. We overcome the data paucity by learning, in a one-shot setup, from a single artist sketch of a given 3D shape and a best matching analytical camera view of the same shape. We match the contours of the depicted shape in this view to corresponding artist strokes. We then learn a spatially continuous local perspective *deviation* function that modifies the camera perspective projecting the contours to their corresponding strokes while retaining key geometric properties that artists strive to preserve when depicting 3D content. We leverage the observation that artists employ similar perspectives when depicting shapes from slightly different view angles to algorithmically augment our training data. First, we use the perspective function learned from the single example to generate more human-like contour renders from nearby views; then, we pair these renders with the analytical camera contours from these views and use these pairs as additional training data. The resulting learned perspective functions are well aligned with the training sketch perspectives and are consistent across views. We compare our results to potential alternatives, demonstrating the superiority of the proposed approach, and showcasing applications that benefit from our learned human perspective.

Additional Key Words and Phrases: human perspective deviation, sketching, matching, perspective, drawing, one-shot learning

1 INTRODUCTION

Line drawings, or sketches, are a simple and powerful medium for conveying shapes between humans [Eissen and Steur 2008, 2011]. As such, they can potentially serve as an effective bidirectional method for communicating shape between a human and a computer [Sutherland 1964], both allowing a computer to communicate stored 3D shape to human observers and allowing humans to use sketches as a way to communicate their imagined shapes to modeling software. In practice, however, computer generated sketches lack the communication power of human ones, and while human observers can easily mentally parse a line drawing and ideate the artist-intended shape, enabling computers to do the same remains an open problem [Bessmeltsev and Liu 2024].

Line drawings (e.g., Figure 1a) roughly correspond to 2D projections of 3D curves on the surface of the shapes that artists aim to represent. While both the choice of surface curves drawn and the structure of strokes used to depict these curves have been extensively researched (Section 2), the type of *projection* artists employ has not received similar attention. While computer graphics and vision applications typically use an analytical model of projection (single vanishing-point perspective or orthographic projection) [Foley et al. 1996], it had been repeatedly noted [Gombrich 1951; Hertzmann 2022; Singh 2002; Xu et al. 2014] that artist projection approximates but does *not* match this analytical model. Researchers speculate

Authors’ addresses: Jinfan Yang, University of British Columbia, Canada, yangjf@cs.ubc.ca; Leo Foord-Kelcey, University of British Columbia, Canada, leofk@cs.ubc.ca; Suzuran Takikawa, University of British Columbia, Canada, stakikaw@cs.ubc.ca; Nicholas Vining, NVIDIA, University of British Columbia, Canada, nvining@cs.ubc.ca; Niloy Mitra, University College London, United Kingdom, niloym@gmail.com; Alla Sheffer, University of British Columbia, Canada, sheffa@cs.ubc.ca.

that the deviation between artist-employed and analytical perspective models is due to a combination of artists using deliberate distortions as a key mechanism to emphasize essential features and reduce cognitive load, thereby enabling more effective communication [Arnheim 1974; Cole et al. 2008; Olsen et al. 2009; Tory and Moller 2004]; and inherent human imprecision. We refer to this discrepancy between analytical and human-drawn perspectives as *human perspective deviation*. Although this deviation has been consistently observed, we are unaware of any principled effort to model or quantitatively analyze it. Our work is designed to fill this void.

We propose a novel framework for learning human perspective deviation, and more specifically human deviation present in contour drawings of 3D shapes; we use the term contour loosely to include occluding contours, sharp features, and other prominent surface curves. The first challenge we face in developing this framework, is that there is no unified perceptual model of artist perspective deviation on which we can draw. We address this challenge by adopting a learning-based approach. We note that while artist perspective deviates from analytical orthographic or pinhole perspective, this deviation is typically not very large, as artists are trained to use approximate pinhole perspective in their drawings [Eissen and Steur 2008; Singh 2002; Tolba et al. 1999]. We therefore use pairs of artist sketches and renders of analytically projected contours of the artist depicted shapes as training data (Figure 1ab). We align the render camera parameters to best match the artist sketches. We then algorithmically match the rendered projected contours to artist strokes and use these correspondences to learn a *perspective deviation* function that maps contours to their matching strokes. We seek a function that generalizes across views and shapes, and design our loss function to be consistent with observations about human perspective choices. We model perspective deviation using a spatially varying multiplicative matrix that adjusts the analytical projection matrix; specifically, we use a multi-layer perceptron (MLP) to define, for every point in 3D space, an associated deviation matrix.

Our second major challenge is data sparsity. While we demonstrate our method on a corpus of 101 pairs of artist sketches and corresponding shapes (Section 5), this data is far from sufficient to learn a universal deviation function for translating from analytical perspective to human perspectives. Moreover, both our observations and prior work [Agrawala et al. 2000; Hertzmann 2022; Kapkin 2020; Singh 2002] suggest not only that different artists make different perspective choices, but that the same artist may make different choices based on different content. Naively optimizing for a deviation function that works across multiple examples in our corpus results in a meaningless average deviation that does not capture the choices artists made in individual examples (Section 5). We therefore develop a method to learn perspective deviation in a one-shot fashion from a single input, namely a paired artist sketch and corresponding contour rendering of the same 3D shape. To generalize the output perspective deviation across multiple camera views, we use a self-augmentation process where we first learn artistic deviation from this input alone. We then use this learned deviation to generate additional synthetic training examples by rendering the shape’s contours from similar views and generating pseudo-artistic drawings by applying the just-learned deviation to these contours.

Finally, we learn a deviation function across both the original and synthetic training examples (Figure 1c).

We evaluate our method across 101 sketches, and show the results throughout the paper and the supplementary. Our outputs retain the perspective of the input sketches when applied to same and different camera views (e.g., Figure 1d), and translate across similar shapes (e.g., Figure 1e). As no prior work on learning of human perspective exists, we ablate our method by comparing our outputs to those of methods that can potentially be used to capture this perspective. As our comparisons show, none of these alternatives capture or replicate human perspective. We further ablate our algorithmic choices and demonstrate the applicability of our method for NPR applications. Finally, we evaluate the degree to which our outputs appear human-like via a perceptual study; participants judged our projected contours as significantly more likely to have been drawn by a human than analytically projected ones.

Our main contribution is the first principled attempt to model and learn human perspective deviation from single training samples. In the process of doing so, we contribute to the understanding of human employed perspective in line drawings and identify the relevant factors behind modeling human perspective deviation. Further, we demonstrate how to generalized learned perspective deviation across views and also across (similar) shapes. Beyond addressing the technical challenge of modeling perspective deviation for individual artists and inputs, our approach advances the understanding of how computational models can replicate human perception.

2 RELATED WORK

Sketching with Perspective. Analytical, linear, perspective projection is ubiquitously used for precise depiction of 3D content from a given viewpoint in both manually drafted technical drawings and computer generated renders. While using perfect perspective is trivial and natural in computer graphics settings, humans cannot and do not sketch this way. In general, artists are encouraged [Eissen and Steur 2008] to aim for analytic perspective and historically have attempted to accurately reproduce it; for example, it is speculated that the Dutch masters used *camera obscura* to capture perfect perspective [Steadman 2002]. However, various user studies have demonstrated that artists almost never use precise linear perspective for sketching [Koenderink et al. 2016]. Some deviations from precise perspective arise due to faulty estimation [Kemp 1991; Kubovy 1986] while others are the result of artists intentionally using varying (local) perspective [Coleman et al. 2005; Schmidt et al. 2009a; Singh 2002]. Research on human perception of 2D depiction of 3D objects strongly suggests that humans make systematic errors when estimating foreshortened shapes and dimensions even for simple tasks [Koenderink and van Doorn 1991; Nicholls and Kennedy 1995; Reith and Liu 1995; Taylor and Mitchell 1997]. While studies suggest that using scaffolds for guidance [Hennessey et al. 2017; Schmidt et al. 2009a] improves the alignment of artist and analytic perspectives, artists often forego scaffolds when sketching free-hand. Please see [Hertzmann 2022] for a recent discussion on artistic perspective. We are unaware of any prior work that aims to learn and/or model such perspective deviation directly from sketches.

Non-Photorealistic Rendering (NPR). NPR seeks to generate artistic and stylized renderings from 3D models or scenes [Gooch and Gooch 2001; Hertzmann 2010] and typically employ analytic perspective. Many NPR works focus on stylized shading, while others have explored rendering objects as line drawings to effectively conveying shape. The latter research primarily investigates *which* surface curves or contours to draw, e.g. [Cole et al. 2008], and how to *stylize* their 2D projections, e.g. [Hähnlein et al. 2022]. DeCarlo et al. [2003] generate collections of curves that emphasize object features; recent variants (e.g., Hähnlein et al. [2022]) convert CAD sequences to concept sketches, blending geometric precision with stylistic abstractions to emulate human sketches. All above methods explicitly or implicitly rely on traditional, analytical perspective.

Advances in machine learning have opened new possibilities for synthesizing line drawings from 3D shapes, including neural style transfer [Gatys et al. 2016] and image-to-image translation [Isola et al. 2017]. Recently, Liu et al. [2020] have proposed a neural framework for generating contour lines directly from 3D models, showcasing the ability of neural networks to learn artistic cues. Chen et al. [2022] propose neural variants for synthesizing line drawings that simultaneously capture geometric accuracy and semantic meaning. These methods demonstrate the potential of ML for mimicking artistic styles, but often focus on predefined objectives (e.g., edge extraction or style replication). They are mainly trained on synthetic renderings of 3D models using analytical projections, and learn styles rather than human perspective. *None* of these explicitly address the perspective distortion humans naturally introduce. This is particularly evident when comparing NPR outputs with human-drawn sketches (see Section 5 for comparisons).

Sketch Processing. Significant research exists on various purely 2D sketch processing operations, including vectorization (e.g., [Favreau et al. 2016; Simo-Serra et al. 2016; Stanko et al. 2020]) and beautification (e.g., [Fišer et al. 2016; Paulson and Hammond 2008]), and well as various aspects of clean-up, or consolidation, of raw artist sketches [Liu et al. 2023a, 2018, 2015; Van Mossel et al. 2021; Yin et al. 2022]; see [Bessmeltsev and Liu 2024] for a recent survey. The problem we address is orthogonal to those. We successfully train our deviation function on raw, unconsolidated vector sketches.

Sketch-Based Modeling. Sketch-based modeling systems focus on creating 3D models from 2D sketches; see [Bessmeltsev and Liu 2024; Olsen et al. 2009] for comprehensive surveys. Many such systems ignore the problem of perspective entirely, and use 2D contour curves drawn in the image plane as input [Dvorožňák et al. 2020; Li et al. 2018; Nealen et al. 2007; Zhang et al. 2022]; they create 3D geometry by inflating these contours and incorporate depth either by explicit annotation or relying on stroke draw order. These methods target organic shapes and implicitly assume orthographic perspective. Other methods rely on sketched input from multiple views, where artists sketch strokes from different viewpoints onto existing 3D geometry (e.g. [De Paoli and Singh 2015; Igarashi et al. 1999; Kara and Shimada 2007]). Several methods require users to manually specify analytic perspective “scaffolds” to regularize perspective [Schmidt et al. 2009b], or use strokes to define transient construction surfaces to recover 3D curves [Bae et al. 2008].

Works addressing 3D reconstruction from single sketches observe that user inputs have inexact perspective, but seek to correct or sidestep this inexactness by detecting and enforcing different regularization cues [Shao et al. 2012; Xu et al. 2014], construction lines [Gryaditskaya et al. 2020], or local symmetries [Hähnlein et al. 2022]. Notably, as Xu et al. [2014] observe, “the perspective in free-hand sketches is too inexact to meaningfully invert”.

Recent developments have shifted towards data-driven approaches by leveraging 3D datasets, synthetically rendered with a pinhole camera model with either non-photorealistic rendering or manual contour tracing, to create training and test data [Li et al. 2022; Liu et al. 2024, 2023b]. When applied to human sketches, they frequently produce unexpected or inconsistent outputs, highlighting the need for frameworks that explicitly incorporate human perceptual biases (Section 5). Similar data-heavy learning approaches are not applicable in our setting, where only limited training examples exist.

3 OVERVIEW

We leverage prior research on sketching [Coleman et al. 2005; Gryaditskaya et al. 2019; Xu et al. 2014] and sketching tutorials [Eissen and Steur 2008] to identify the core properties of the deviation we seek to capture. Drawing and sketching tutorials teach artists to use analytic (orthographic or perspective) projection when depicting 3D content [Eissen and Steur 2011]. Consequently, while artistic perspective typically deviates from analytic perspective, this deviation is relatively subtle. Some of this deviation is due to the challenges of accurately depicting perspective in freehand drawings, while some of the deviation is intentional. In particular, artists’ choice of perspective often subtly varies across drawings, with parts of the content artists wish to subtly emphasize drawn larger than they would be using analytic projection, or conversely using an exaggerated perspective to make content look farther away than it is [Coleman et al. 2005; Hertzmann 2022]. Based on these observations, we model artists’ perspective as a deviation from a standard pinhole camera projection (we recall that orthographic projection is a special case of perspective with the camera placed at infinity) that smoothly varies across 3D space.

Setup. In computer graphics, projection is handled analytically through the camera projection matrix \mathbf{P} and the modelview matrix \mathbf{M} . For simplicity going forward we refer to the product of these matrices $\mathbf{C} = \mathbf{PM}$ as the camera projection matrix. When applying a perspective projection, any point $\mathbf{p} \in \mathbb{R}^3$ on a 3D shape gets mapped, working in homogeneous coordinates, to $\mathbf{p} \rightarrow \mathbf{C}[\mathbf{p}; 1]$ (here we approximate orthographic perspective as perspective projection with camera at infinity). $\mathbf{C}[\mathbf{p}; 1]$ is converted to 2D points in image space by performing a perspective divide (see [Foley et al. 1996] for details).

We model human perspective deviation as a local multiplicative adaptation of the projection operator. Empirically, we found that human perspective is best modeled in a normalized world coordinate space, and not in image space. We therefore model human perspective at \mathbf{p} as a 4×4 deviation matrix $\mathbf{D}(\mathbf{p})$, and thus we model human perspective as $\mathbf{p} \rightarrow \mathbf{D}(\mathbf{p})\mathbf{C}[\mathbf{p}; 1]$, followed by perspective division by p_w . Input shapes are normalized so their origin is at $(0, 0, 0)$ and

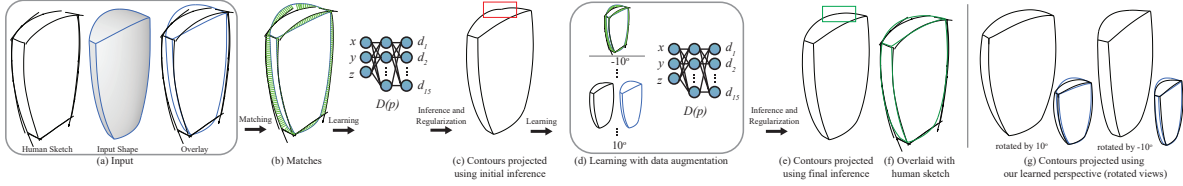


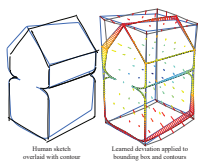
Fig. 2. Algorithm overview: Given an input sketch and corresponding 3D shape in a matching view (a), we match the projected shape contours to artist strokes (b). We then use a two-step process to learn the deviation between the shape and sketch projections (c-e): we use the matches to obtain an initial deviation function $D(p)$ that balances satisfying these matches against adherence to core deviation properties; we apply the learned deviation to the input contours (d); we augment our learning data with synthetic sketch/shape pair and re-learn a deviation that best matches augmented training set (d,e). The contours projected using ours align with the artist’s strokes (f). Applying our learned perspective (e) to different camera views generates plausible projections (g).

the shape is within the $[-1, 1]^3$ unit box; thus we parameterize D queried based on the normalized world coordinates.

We represent D as an MLP that takes in 3D (normalized) coordinate information and outputs 15 values. We map these values to a 4×4 matrix, with the last element always being 1. Given this one-to-one relation, we use D to represent, based on context, both the human perspective matrix as well as the MLP.

Deviation Properties. Based on the observations above we expect our learned deviation functions D to have the following properties. Deviation should change gradually and slowly across the input shapes, and should be similar across similar views. Rather than requiring the deviation to be minimal across the board (for example, having D be close to identity), we qualify it to preserve core properties of the projections of the depicted curves such as slope and curve shape preservation. This choice is motivated by prior research on sketch analysis [Shao et al. 2012; Xu et al. 2014] that suggests that artists seek to preserve these properties in their sketches, while at the same time allowing for spatial drift (having sketched strokes some distance apart from the camera projections of the surface curves they depict) and subtle uniform scaling. These observations are confirmed by analysing our training corpus, and illustrated by the overlays of artist sketches and 3D contours projected using their best matching pinhole camera views (Figures 1b, 2a and 5b).

4 ALGORITHM



We design our algorithm to learn the deviation matrix $D(p)$, in a single-shot fashion, from a source sketch along with its corresponding 3D object and an estimated camera matrix that best aligns the sketch and camera views. A representative example of the deviation learned and its application to a set of contours are shown in the inset. We break the task into the following stages (Figure 2):

(i) matching between sketched strokes and analytically projected 3D shape contour curves using an estimated camera; (ii) learning, using the mapping between matched contour and stroke vertices, a human perspective deviation function, encoded as a spatially-conditioned MLP; (iii) post-regularization, after applying the learned perspective deviation, for predicting sketches across view and shape variations; and (iv) self-augmentation to create additional data to retrain the MLP to better align $D(p)$ with our global priors and better generalize to nearby camera settings. Given each new shape and camera

combination, we apply the resulting learned perspective deviation, followed by regularization (Figure 2, right).

Pre-Processing. Using the calibrated camera data for the input object, we render its occluding contours, sharp features, and surface boundaries; for conciseness, we refer to all these curves as *contours* throughout. We vectorize this projected contour render and normalize its bounding box to lie in the range $[-1, 1]^2$. We segment each contour into subcurves with smoothly changing curvature (clothoids/arcs/lines) and resample each curve using a fixed sampling rate (we denote the sampling interval length as l). We use our camera information to obtain depth and 3D coordinates for each projected curve vertex p by reverse projecting it from normalized 2D space back to 3D. We expect input sketches to be in vector form, and vectorize them if they are not. We normalize the dimensions of each sketch, and segment and resample its strokes; see the supplemental material for pre-processing details. In the following, unless stated otherwise, the term *curve* refers to a resampled projected contour curve and the term *stroke* refers to a resampled sketch stroke.

Notation. We use \hat{p} as the 3D locations of the 2D contour vertices p . We assume all 3D vertices are written as homogenous coordinates (i.e., $\hat{p} = (x, y, z, w)$ with $w = 1$), and all matrices, unless stated otherwise, are 4×4 homogenous transformation matrices. Given a vertex \hat{p} and a projection matrix D , the function $\text{proj}(\hat{p}, D)$ is the 2D vertex computed by taking the matrix-vector product $DC \cdot \hat{p}$ in homogenous coordinates, and applying the perspective divide.

4.1 Matching Contour Curves to Sketch Strokes

First, we establish correspondences between vertices on the projected contour curves and vertices on the vectorized human sketch strokes. Our challenge in computing these correspondences is that they are not one-to-one (Fig 2b). Sketches may contain strokes, or portions of strokes, with no matching contours, due to over-ketching [Van Mossel et al. 2021]; object curves may be depicted using multiple strokes, and some of the curve vertices may not have corresponding stroke locations.

Intuitively, we seek to match contour vertices to nearby stroke vertices with similar tangents. While we do not expect exact one-to-one contour to stroke matches, we generally expect segments formed by consecutive contour vertices to match pairs of stroke vertices that form roughly parallel line segments. We formulate our

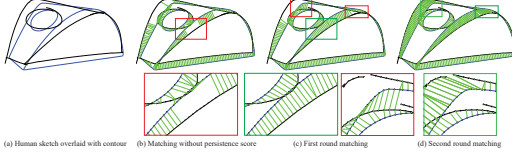


Fig. 3. Given the sketch strokes (black) and projected contours (blue), we seek for the artist intended matches between them. Using only vertex-to-vertex matching scores produces locally optimal but globally poor matches (b); using our HMM formulation, we obtain better per curve matches (c), but multiple curves can match the same stroke (see inset zoom). Our second matching step resolved these undesirable many-to-one matches (d).

matching problem as an instance of the classical Hidden Markov Model (HMM) problem [Yoon 2009].

Given a contour curve $S = \{p_0, \dots, p_n\}$, we first form, for each contour vertex p_i , a candidate set of potential matching stroke vertices $Q = \{q_0, \dots, q_m\}$ on the human sketch based on the distance between these vertices in 2D image space. We then evaluate potential matches $(p_i, q_{j(i)})$ using a combined vertex-to-vertex *compatibility* score $S^v(p_i, q_{j(i)})$ and a *persistence* score $S^e(p_i, p_{i+1}, q_{j(i)}, q_{j(i+1)})$ that assesses compatibility between potential matches of consecutive curve vertices. Using the classical HMM formulation, the overall score given by matching the vertices of S to the vertices of Q is:

$$M(S, Q) = \prod_i S^v(p_i, q_i) S^e(p_i, p_{i+1}, q_i, q_{i+1}). \quad (1)$$

Using a product rather than a sum discourages outlier matches.

We compute the matches for each curve that maximize $M(S, Q)$ using the Viterbi algorithm [1967]. To obtain a valid solution, we exclude any vertices with empty matching candidate sets, and any edges emanating from such vertices, from the per-curve score.

Vertex-to-Vertex Matching Score. Given a paired curve vertex p and stroke vertex q , we define the score of using q as the match of p as a function of two terms, designed to be on the same scale.

$$d_a = \|p - q\|_2. \quad (2)$$

$$d_t = 1 - |\mathcal{T}_S(p) \cdot \mathcal{T}_Q(q)|. \quad (3)$$

The first term is the absolute distance between them, while the second term measures the similarity of the vertices' tangents and encourages matches that have similar orientations: Here, $\mathcal{T}_S(p)$ is the normalized tangent vector of S at p (respectively for Q at q). The overall score for matching q to p is thus:

$$S^v(p, q) = e^{-(d_a + d_t)^2 / 2\sigma_1^2}. \quad (4)$$

To support sketches with large perspective deviation, we set σ_1 to be a fairly large value $\sigma_1 = 10l$ (where l is the curve and stroke sampling density), ensuring that the score does not drop too fast.

Persistence Score. We seek to promote consecutive vertices along a given curve to match similarly consecutive stroke vertices, while supporting matches where a curve may correspond to multiple artist strokes or stroke sections. We thus formulate persistence purely geometrically, and prioritize matching contour edges to pairs of vertices where the line connecting these vertices has similar length and orientation to the edge ones. Given a pair of consecutive vertices

p_i and p_{i+1} potentially matching a pair of vertices $q_{j(i)}$ and $q_{j(i+1)}$ respectively, we measure persistence $S^e(p_{i+1}, q_i | q_{i+1})$ as:

$$\begin{aligned} d_p &= \|(p_{i+1} - p_i) - (q_{j(i+1)} - q_{j(i)})\|_2 \\ S^e(p_{i+1}, q_i | q_{i+1}) &= e^{-(d_p)^2 / 2\sigma_2^2}. \end{aligned} \quad (5)$$

While we expect different contours to be depicted using different strokes, enforcing global matching constraints would dramatically increase matching complexity. Instead, we compute matches independently for each contour curve. We then apply a second round of matching to resolve cases where multiple curves or portions of curves are matched to the same stroke/stroke portion (Fig 3c). We first identify vertices from different curves that match the same stroke vertex q . We then do another matching round, where for these conflicted curve vertices we double the distance range to search in when finding candidate sets and exclude their previously matched stroke vertices from the candidate set. For each curve vertex in conflict, we then assign either its first round stroke match, or its new second round match, depending on which solution minimizes its score (Equation (4)), see Figure 3d.

4.2 Learning Human Perspective

We use the results of the matching to learn a deviation matrix that satisfies the smoothness and shape preservation properties identified above, and that approximately projects the original 3D locations \hat{p}_i of the projected contour vertices p_i to their matching 2D stroke vertices $q_{j(i)}$. Specifically, we learn an MLP that takes as input the coordinate \hat{p} in the normalized 3D space of our sketch $[-1..1]^3$ and outputs a deviation matrix $\mathbf{D}_{\hat{p}}$ satisfying these requirements.

Formally, let $P = \{p_1, p_2, \dots, p_n\}$ be all vertices on the projected contours; let $Q = \{q_1, q_2, \dots, q_n\}$ be the matched vertices in the human vector sketch; for notational simplicity, we replace $q_{j(i)}$ with q_i . By abuse of notation, we identify each vertex p_i with a distortion matrix \mathbf{D}_i that is the output of the MLP at \hat{p}_i (i.e., $\mathbf{D}_i = \mathbf{D}(\hat{p}_i)$), and denote the collection of all such matrices $\mathbf{D} = \{\mathbf{D}_1, \mathbf{D}_2, \dots, \mathbf{D}_n\}$.

Confidence. While we generally seek to project 3D contour vertices \hat{p}_i to their stroke matches q_i , the matches we compute may be imperfect due to factors such as oversketching (e.g., top of shampoo bottle in Figure 2b). We therefore associate confidence values α_i with each matched pair. We base these values on the difference between intrinsic contour and stroke shape at the respective 2D vertices. Since artist sketches tend to preserve curve shape, mismatches between local curve shapes point to potential matching errors. For simplicity, we use polyline angles at p_i and q_i as proxy for shape. Let $e_i = (p_i - p_{i-1})$ and $e_{i+1} = (p_{i+1} - p_i)$; $e'_i = (q_i - q_{i-1})$ and $e'_{i+1} = (q_{i+1} - q_i)$. We then define the curvature difference between the projected contour and the human sketch at i as:

$$\Delta_i = \arccos\left(\frac{e_i \cdot e_{i+1}}{\|e_i\| \|e_{i+1}\|}\right) - \arccos\left(\frac{e'_i \cdot e'_{i+1}}{\|e'_i\| \|e'_{i+1}\|}\right) \quad (6)$$

and the overall confidence as (used later in the loss):

$$\alpha_i = e^{-\Delta_i^2 / 2\sigma_2^2}. \quad (7)$$

We set $\sigma_2 = \pi/9$ using the three sigma rule, so that once the angular difference approaches $3\sigma_2 = \pi/3$ the confidence drops to near zero.

Overall Loss. Our loss function is a weighted combination:

$$L(D) = w_1 \cdot L_{data} + w_2 \cdot L_{shape} + w_3 \cdot L_{slope} + w_4 \cdot L_S + w_5 \cdot L_{depth}. \quad (8)$$

The first term aims to project 3D contour vertices close to their matching stroke vertices; the second and third terms aim to preserve shape and slopes; the fourth term explicitly preserves deviation smoothness; the last term seeks to avoid depth instabilities. We set $w_1 = 0.001$, $w_2 = 10$, $w_3 = w_4 = 1$, $w_5 = 10^{-5}$. This prioritises shape preservation above all other properties, and prioritizes our general priors about deviation above the data term. A tiny weight is sufficient to avoid depth instabilities.

Data Loss (L_{data}). The term moves projected contour vertices $\text{proj}(\hat{p}_i, \mathbf{D}_i)$ toward their counterparts q_i on the human sketch, as:

$$L_{data} = \frac{1}{\text{avg}_l} \frac{1}{n} \sum_{i \in n} \alpha_i \|\text{proj}(\hat{p}_i, \mathbf{D}_i) - q_i\|_1 \quad (9)$$

where $\text{avg}_l = \frac{1}{n} \sum_{i \in n} \|p_i - q_i\|_1 + l$. We normalize each individual term by the confidence of the individual match, and normalize the entire data term by the average distance between matching vertices (we add l to avoid division by zero for perfect matches).

Shape Loss (L_A). The term aims to ensure our deviation preserves curve shape penalizing non-uniform scale and shear,

$$L_{shape} = \sum_{i \in V} \sum_{j, k \in N(i); j \neq k} (1 - \alpha + \epsilon) \left(\|\text{proj}(\hat{p}_k, \mathbf{D}_k) - \text{proj}(\hat{p}_i, \mathbf{D}_i)\| - (R_i \frac{\|p_k - p_i\|}{\|p_j - p_i\|} (\text{proj}(\hat{p}_j, \mathbf{D}_j) - \text{proj}(\hat{p}_i, \mathbf{D}_i))) \right)^2. \quad (10)$$

Here V is the set of all vertices lying on the interior of projected contour curves, $\epsilon = 0.1$ and $N(i)$ are all neighbouring vertices of the vertex i . α is the minimum confidence value α_i of the three consecutive vertices p_j, p_i, p_k forming the two edges; R_i is the rotation matrix in 2D space that rotates the vector $p_j - p_i$ to $p_k - p_i$.

Slope Loss (L_{slope}). The term aims to preserve the slopes of the projected contours under our learned deviation

$$L_{slope} = \frac{1}{n-1} \sum_{i=2}^n \left(\hat{n}_i \cdot \frac{\|\text{proj}(\hat{p}_i, \mathbf{D}_i) - \text{proj}(\hat{p}_{i-1}, \mathbf{D}_{i-1})\|}{\|p_i - p_{i-1}\|} \right)^2 \quad (11)$$

where \hat{n}_i is the 2D normal of the projected contour edge $(p_i - p_{i-1})$.

Smoothness Loss (L_S). The term encourages smooth changes in the distortion matrix across view space and is computed over a set of points \hat{S} containing all contour vertices \hat{p} as well as the vertices of a dense grid spanning our 3D domain box $[-1, 1]^3$. In particular, given two vertices $s_i \in \hat{S}$ and $s_j \in \hat{S}$, we expect \mathbf{D}_i and \mathbf{D}_j to be more similar the closer the two vertices are. Hence, we use:

$$L_S = \frac{1}{|\hat{S}|} \sum_{s_i \in \hat{S}} \sum_{s_j \in \hat{S}, i \neq j} e^{-\frac{(\|s_i - s_j\|)^2}{2\sigma_1^2}} \|\mathbf{D}_i - \mathbf{D}_j\|_{\text{Frob}}. \quad (12)$$

Depth Consistency Loss (L_{depth}). In post-projection space, inverting the direction of the depth axis either globally or locally has no impact on the 2D projection. While not observable for an individual view, such inversion results in inconsistent results when the camera

is rotated. We avoid inversions by adding a depth consistency term to preserve the relative depth of the transformed vertices, as:

$$L_{depth} = \sum_{i, j \in n, i \neq j} w_{ij} \|D_i C \hat{p}_i^z - D_j C \hat{p}_j^z - (\hat{p}_i^z - \hat{p}_j^z)\| \quad (13)$$

where \hat{p}_j^z is the depth of the vertices \hat{p}_j along the viewspace z-axis.

4.3 Inference and Regularization

We use our learned MLP to render any set of 3D surface curves from a given camera view. Specifically, we use the learned MLP to project 3D surface vertices \hat{p} to image space, by first multiplying each vertex by the user specified camera matrix C , multiplying the result by $D(\hat{p})$ and applying perspective divide (Figure 2c). We then apply a post-inference regularization step (see supplemental material).

4.4 Self-Augmentation for Refined Learning

Our initial learning is based on a single set of potentially imperfect contour-to-stroke matches. As such, it is not necessarily smooth and bakes in matching imperfections (e.g., top of the shampoo in Figure 2) even after regularization. We improve our learned deviation function by repeating the learning step using augmented data. To this end, we use our inference method above to generate new pairs of contours and matching deviated contours. In our experiment, this involves rotating the object by $[-5, -4, \dots, 5]$ degrees around the vertical axis. We render the contours of the rotated shape twice, once using an analytical camera matrix C_r and once using our inference method that multiplies C_r by our learned deviation matrix \mathbf{D} , then regularizes the output. We pre-process each pair of outputs as described before, and use the depths of the originating 3D contour vertices to match them. We then use these 11 pairs, plus the original contours and sketch, as training data for another learning step using the same MLP architecture and loss functions as the initial phase. We repeat this process, this time augmenting the data by rotating the object by $[-10, 10]$. This iterative process enables the model to capture and enhance visual consistency across different views.

5 RESULTS

We test our method on 101 sketches (96 from OpenSketch [Gryaditskaya et al. 2019] across 6 artists and 9 shapes, and newly collected cube sketches from 5 artists). In addition to examples shown in the paper, we include results trained on all other sketches in the supplementary material. We show human perspective (sketches, ours, other methods, and ablations) in *black*, and render the projected contours of the original 3D models under analytical perspective, from the original camera, in *blue*.

Figure 5d shows a gallery of projected contours rendered from same and novel viewpoints with our learned perspective. For each artist, we learn perspective from a given sketch/contour pair and fixed camera, and then ‘rotate’ the sketch by rotating the viewpoint, reprojecting the contours from that viewpoint, then applying our learned perspective. Our rotated outputs incorporate the learned artist perspective, even from novel very different viewpoints.

Visual Comparison to Prior Work. While no prior work we are aware of, attempted to learn human perspective, we compare our results to those of methods that solve potentially similar tasks.

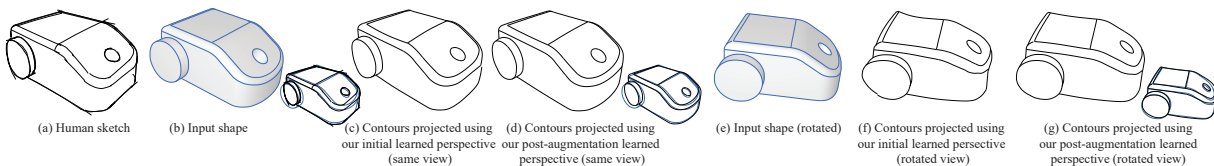


Fig. 4. Augmentation impact (left to right): (a) input sketch; (b) depicted 3D object in matching view (inset shows contour and sketch overlay); (c) same view inference output using first learned MLP; (d) same view inference output using data augmented MLP, alternative view (e) inference output using first learned MLP (f), alternative view inference output using data augmented MLP (g). The impact of augmentation is most notable for further away camera views.

We first compare our method to Zero123 [Liu et al. 2023b], a representative approach for novel view synthesis. In theory, given an input sketch, such methods may be able to reproduce the sketched content appropriately rotated and retain the artist’s perspective. As fig. 7 shows this is unfortunately not the case: the pre-trained Zero123 model fails to generate meaningful results on many inputs. Additional examples are shown in the supplementary.

We compare our learned perspective results, both under original and novel viewpoints, to those produced by [Chan et al. 2022], a state-of-the-art method for generating stylized line drawings from images. Their model was trained on OpenSketch-style data, aligning with our human sketch dataset. Their method focuses on the stylization, and as our experiments (Figure 6) confirm, does *not* change the input perspective. As shown in Figure 6, when overlaying their outputs with the input projected vector contours, they are perfectly matched. This result holds true whether the input to their method is a shaded (Figure 6,b) or contour (Figure 6,c) render. In contrast contours rendered by our method reproduce the perspective deviation present in the artist sketches.

Lastly we compare our outputs to those obtained by training Pix2Pix [Isola et al. 2017] on our paired sketch and contour corpus, appropriately rasterized did not learn the human perspective and instead. Rather than learning perspective deviation, the resulting model produces somewhat messy, no longer stroke based, stylized outputs which retained the original analytic perspective when presented with same view or rotated contours.

In all cases, our experiments show that these alternative methods fail to reproduce human perspective deviation, showcasing both the need for a method that explicitly aims to learn perspective deviation and our method’s ability to do so (see also supplementary).

Perceptual Study. We assess the degree to which our learned deviation makes contour drawings appear more human like via a user study. Participants were shown same view contours projected using both analytical and our learned perspective, and were asked to assess which output was “more likely to have been drawn by a human”. Participants rated our outputs as more human-like 71% of the time, the analytical contours as more likely to be human like 12% of the time, both equally likely 8%, neither likely 9%. This confirms the suitability of our method for applications such as NPR or sketch based modeling where users seek human-like renders of surface curves. See supplementary for details.

Ablations. We compare our learned perspective against potential baselines. A naive baseline is to use a single deviation matrix D

to model perspective deviation throughout (Figure 9b); or alternatively, a small finite set of perspective deviation matrices positioned at evenly distributed fixed points and linearly interpolated everywhere else (Figure 9c; 9 matrices). Both solutions fail to account for the locality of human deviation. In our experiments, the matrices learned with both setups tended to be extremely close to identity. Our pointwise alternative correctly learns local human deviation (Figure 9d).

We validate our decision to use a one-shot learning approach by training our perspective MLP on a corpus consisting of all inputs drawn by the same artist (Figure 10,left); and all artists’ sketches of the same object (Figure 10,right). Learning one artists’ perspective across multiple shapes does not fully capture the perspective of the original human sketch. Training the same shape across multiple artist sketches causes each artists’ unique perspective to be lost, and produces a result very similar to the input shape contours.

Applications. Figure 1d demonstrates that our learned perspective can be transferred to other objects (Figure 1). Our learned perspective can be part of a larger stylization or NPR pipeline. Figure 11bd shows our learned perspective applied to contours that are subsequently restyled with the *CAD2Sketch* style transfer pipeline [Hähnlein et al. 2022]. Figure 11h shows that our learned perspective can be applied to other classes of surface curves; in this case, we apply it to a coarse quad mesh [Nuvoli et al. 2019; Pietroni et al. 2021].

6 CONCLUSION

We presented the first method to model and learn the perspective projection humans use when creating line drawings. Our approach overcomes the paucity of suitable training data by using a one-shot framework and produces convincing outputs, when trained from single pairs of a 3D shape and its sketch. We thoroughly evaluate our design choices and provide extensive comparisons to relevant prior art, demonstrating the superiority of our selected approach.

Limitations and Future Work. A potential drawback of learning from a single example is that the deviation function we learn may be *too* artist- or shape-specific. Unfortunately, learning a single deviation function from several examples leads to undesirable expressivity loss (Figure 10), Applying methods that learn a space of deviation functions rather than a single one would mitigate this problem, but would unfortunately require orders of magnitude larger datasets than we currently have. It would be interesting to analyze the similarities and differences between the functions we learn across different shapes and artists and to use the results of this

analysis to select or compute the visually best deviation for a new input, or allow users to navigate the space of possible deviations.

While we targeted production sketches of CAD/human-made content, it would be interesting to explore how well our approach generalizes to sketches of other content. Perhaps the most exciting avenue for leveraging our method's outputs is using them as a basis for a method capable of inverting artist deviation, i.e. taking free-hand sketches and producing 2D curves that are the *analytic* projection of artist intended 3D surface curves. The outputs of this method could be used to accurately recover the depicted 3D content, providing a big step toward robust sketch-based 3D modeling.

REFERENCES

- Maneesh Agrawala, Denis Zorin, and Tamara Munzner. 2000. Artistic Multiprojection Rendering. *Eurographics Rendering Workshop 2000* 2000, 125–136. https://doi.org/10.1007/978-3-7091-6303-0_12
- Rudolf Arnheim. 1974. *Art and Visual Perception: A Psychology of the Creative Eye*. University of California Press.
- Seok-Hyung Bae, Ravin Balakrishnan, and Karan Singh. 2008. ILoveSketch: as-natural-as-possible sketching system for creating 3d curve models. In *Proceedings of the 21st annual ACM symposium on User interface software and technology*. 151–160.
- Mikhail Bessmeltsev and Chenxi Liu. 2024. Fundamentals and Applications of Sketch Processing. In *Symposium on Graphics Processing (SGP 2024) Course*. <https://school.geometryprocessing.org/summerschool-2024/>
- Caroline Chan, Frédo Durand, and Phillip Isola. 2022. Learning to generate line drawings that convey geometry and semantics. In *CVPR*.
- Forrester Cole, Aleksey Golovinskiy, Alex Limpaecher, Heather Stoddart Barros, Adam Finkelstein, Thomas Funkhouser, and Szymon Rusinkiewicz. 2008. Where Do People Draw Lines? *ACM Transactions on Graphics (Proc. SIGGRAPH)* 27, 3 (Aug. 2008).
- Patrick Coleman, Karan Singh, Leon Barrett, Nisha Sudarsanam, and Cindy Grimm. 2005. 3D screen-space widgets for non-linear projection. In *Proc. Computer Graphics and Interactive Techniques (GRAPHITE '05)*. 221–228.
- Chris De Paoli and Karan Singh. 2015. SecondSkin: sketch-based construction of layered 3D models. *ACM Transactions on Graphics (TOG)* 34, 4 (2015), 1–10.
- Doug DeCarlo, Adam Finkelstein, Szymon Rusinkiewicz, and Anthony Santella. 2003. Suggestive Contours for Conveying Shape. *ACM Transactions on Graphics (Proc. SIGGRAPH)* 22, 3 (jul 2003), 848–855.
- Marek Dvorožňák, Daniel Šýkora, Cassidy Curtis, Brian Curless, Olga Sorkine-Hornung, and David Salesin. 2020. Monster Mash: A Single-View Approach to Casual 3D Modeling and Animation. *ACM Transactions on Graphics (proceedings of SIGGRAPH ASIA)* 39, 6, Article 214 (2020).
- Koos Eissen and Roselien Steur. 2008. *Sketching: Drawing Techniques for Product Designers*. Bis Publishers.
- Koos Eissen and Roselien Steur. 2011. *Sketching: The Basics*. Bis Publishers.
- Jean-Dominique Favreau, Florent Lafarge, and Adrien Bousseau. 2016. Fidelity vs. simplicity: a global approach to line drawing vectorization. *ACM Trans. Graph.* 35, 4, Article 120 (July 2016), 10 pages. <https://doi.org/10.1145/2897824.2925946>
- Jakub Fiser, Paul Asente, Stephen Schiller, and Daniel Šýkora. 2016. Advanced drawing beautification with ShipShape. *Comput. Graph.* 56, C (May 2016), 46–58. <https://doi.org/10.1016/j.cag.2016.02.003>
- James D. Foley, Andries van Dam, Steven K. Feiner, and John F. Hughes. 1996. *Computer Graphics: Principles and Practice* (2nd ed.). Addison-Wesley, Reading, MA.
- Leon A. Gatys, Alexander S. Ecker, and Matthias Bethge. 2016. Image Style Transfer Using Convolutional Neural Networks. In *2016 IEEE Conference on Computer Vision and Pattern Recognition (CVPR)*. 2414–2423. <https://doi.org/10.1109/CVPR.2016.265>
- E. H. Gombrich. 1951. The Story of Art. *Journal of Aesthetics and Art Criticism* 9, 4 (1951), 339–340. <https://doi.org/10.2307/426517>
- Bruce Gooch and Amy Gooch. 2001. *Non-Photorealistic Rendering*. A. K. Peters, Ltd., USA.
- Yulia Gryaditskaya, Felix Hähnlein, Chenxi Liu, Alla Sheffer, and Adrien Bousseau. 2020. Lifting Freehand Concept Sketches into 3D. *ACM Transactions on Graphics (Proc. SIGGRAPH Asia)* (2020).
- Yulia Gryaditskaya, Mark Sypsteyn, Jan Willem Hoftijzer, Sylvia Pont, Frédo Durand, and Adrien Bousseau. 2019. OpenSketch: A Richly-Annotated Dataset of Product Design Sketches. *ACM Transactions on Graphics (Proc. SIGGRAPH Asia)* 38 (11 2019).
- Felix Hähnlein, Yulia Gryaditskaya, Alla Sheffer, and Adrien Bousseau. 2022. Symmetry-driven 3D reconstruction from concept sketches. In *ACM SIGGRAPH 2022 Conference Proceedings*. 1–8.
- Felix Hähnlein, Changjian Li, Niloy J. Mitra, and Adrien Bousseau. 2022. CAD2Sketch: Generating Concept Sketches from CAD Sequences. *ACM Trans. Graph.* 41, 6, Article 279 (Nov. 2022), 18 pages. <https://doi.org/10.1145/3550454.3555488>
- James W. Hennessey, Han Liu, Holger Winnemöller, Mira Dontcheva, and Niloy J. Mitra. 2017. How2Sketch: Generating Easy-To-Follow Tutorials for Sketching 3D Objects. *Symposium on Interactive 3D Graphics and Games* (2017).
- Aaron Hertzmann. 2010. Non-Photorealistic Rendering and the science of art. In *Proc. International Symposium on Non-Photorealistic Animation and Rendering (Anney, France) (NPAR '10)*. 147–157.
- Aaron Hertzmann. 2022. The choices hidden in photography. *Journal of Vision* 22, 11 (2022), 10. <https://doi.org/10.1167/jov.22.11.10>
- Takeo Igarashi, Satoshi Matsuoka, and Hidehiko Tanaka. 1999. Teddy: a sketching interface for 3D freeform design. In *Proceedings of the 26th Annual Conference on Computer Graphics and Interactive Techniques (SIGGRAPH '99)*. ACM Press/Addison-Wesley Publishing Co., USA, 409–416.
- Phillip Isola, Jun-Yan Zhu, Tinghui Zhou, and Alexei A Efros. 2017. Image-to-Image Translation with Conditional Adversarial Networks. *CVPR* (2017).
- Engin Kapkın. 2020. Perception of Perspective Drawings: A Contention on the Principle of Choosing Eye-Levels and View-Angles. *The Design Journal* 23, 4 (2020), 621–637.
- Levent Burak Kara and Kenji Shimada. 2007. Sketch-based 3D-shape creation for industrial styling design. *IEEE Computer Graphics and Applications* 27, 1 (2007), 60–71.
- M. Kemp. 1991. The Science of Art – Optical Themes in Western Art from Brunelleschi to Seurat. 617–619 pages.
- Jan Koenderink, Andrea van Doorn, Baingio Pinna, and Robert Pepperell. 2016. On right and wrong drawings. *Art and Perception* (9 2016).
- Jan J. Koenderink and Andrea J. van Doorn. 1991. Affine structure from motion. *J. Opt. Soc. Am. A* 8, 2 (Feb 1991), 377–385.
- Michael Kubovy. 1986. *The Psychology of Perspective and Renaissance Art*. Cambridge University Press, Cambridge, UK.
- Changjian Li, Hao Pan, Adrien Bousseau, and Niloy J Mitra. 2022. Free2cad: Parsing freehand drawings into cad commands. *ACM Transactions on Graphics (TOG)* 41, 4 (2022), 1–16.
- Changjian Li, Hao Pan, Yang Liu, Alla Sheffer, and Wenping Wang. 2018. Robust Flow-Guided Neural Prediction for Sketch-Based Freeform Surface Modeling. *ACM Trans. Graph. (SIGGRAPH ASIA)* 37, 6 (2018), 238:1–238:12. <https://doi.org/10.1145/3272127.3275051>
- Chenxi Liu, Toshiaki Aoki, Mikhail Bessmeltsev, and Alla Sheffer. 2023a. StripMaker: Perception-Driven Learned Vector Sketch Consolidation. *ACM Trans. Graph.* 42, 4, Article 55 (jul 2023), 15 pages. <https://doi.org/10.1145/3592130>
- Chenxi Liu, Enrique Rosales, and Alla Sheffer. 2018. StrokeAggregator: Consolidating Raw Sketches into Artist-Intended Curve Drawings. *ACM Transaction on Graphics* 37, 4 (2018). <https://doi.org/10.1145/3197517.3201314>
- Difan Liu, Mohamed Nabail, Aaron Hertzmann, and Evangelos Kalogerakis. 2020. Neural Contours: Learning to Draw Lines from 3D Shapes. In *IEEE/CVF Conference on Computer Vision and Pattern Recognition (CVPR)*.
- Feng-Lin Liu, Hongbo Fu, Yu-Kun Lai, and Lin Gao. 2024. SketchDream: Sketch-based Text-To-3D Generation and Editing. *ACM Trans. Graph.* 43, 4, Article 44 (July 2024), 13 pages. <https://doi.org/10.1145/3658120>
- Ruoshi Liu, Rundui Wu, Basile Van Hoorick, Pavel Tokmakov, Sergey Zakharov, and Carl Vondrick. 2023b. Zero-1-to-3: Zero-shot One Image to 3D Object. arXiv:2303.11328 [cs.CV]
- Xueting Liu, Tien-Tsin Wong, and Pheng-Ann Heng. 2015. Closure-aware Sketch Simplification. *ACM Transactions on Graphics (SIGGRAPH Asia 2015 issue)* 34, 6 (November 2015), 168:1–168:10.
- Andrew Nealen, Takeo Igarashi, Olga Sorkine, and Marc Alexa. 2007. FiberMesh: Designing Freeform Surfaces with 3D Curves. *ACM Transactions on Graphics (Proceedings of ACM SIGGRAPH)* 26, 3 (2007), article no. 41.
- Andrea L Nicholls and John M Kennedy. 1995. Foreshortening in Cube Drawings by Children and Adults. *Perception* 24, 12 (1995), 1443–1456. <https://doi.org/10.1068/p241443> PMID: 8734543.
- Stefano Nuvoli, Alex Hernandez, Claudio Esperança, Riccardo Scateni, Paolo Cignoni, and Nico Pietroni. 2019. QuadMixer: Layout Preserving Blending of Quadrilateral Meshes. *ACM Trans. Graph.* 38, 6, Article 180 (nov 2019), 13 pages. <https://doi.org/10.1145/3355089.3356542>
- Luke Olsen, Faramarz F. Samavati, Mario Costa Sousa, and Joaquim A. Jorge. 2009. Sketch-based modeling: A survey. *Computers & Graphics* 33, 1 (2009), 85–103. <https://doi.org/10.1016/j.cag.2008.09.013>
- Brandon Paulson and Tracy Hammond. 2008. Paleosketch: accurate primitive sketch recognition and beautification. In *Proceedings of the 13th international conference on Intelligent user interfaces*. 1–10.
- Nico Pietroni, Stefano Nuvoli, Thomas Alderighi, Paolo Cignoni, and Marco Tarini. 2021. Reliable Feature-Line Driven Quad-Remeshing. *ACM Trans. Graph.* 40, 4, Article 155 (jul 2021), 17 pages. <https://doi.org/10.1145/3450626.3459941>
- Emiel Reith and Chang Hong Liu. 1995. What Hinders Accurate Depiction of Projective Shape? *Perception* 24, 9 (1995), 995–1010. <https://doi.org/10.1068/p240995> PMID: 8552463.
- Ryan Schmidt, Azam Khan, Gord Kurtenbach, and Karan Singh. 2009a. On expert performance in 3D curve-drawing tasks. In *SBIM*. New York, NY, USA, 133–140.

- Ryan Schmidt, Azam Khan, Karan Singh, and Gord Kurtenbach. 2009b. Analytic drawing of 3D scaffolds. *ACM Trans. Graph.* 28, 5 (Dec. 2009), 1–10. <https://doi.org/10.1145/1618452.1618495>
- Cloud Shao, Adrien Bousseau, Alla Sheffer, and Karan Singh. 2012. CrossShade: shading concept sketches using cross-section curves. *ACM Trans. Graph.* 31, 4, Article 45 (July 2012), 11 pages.
- Edgar Simo-Serra, Satoshi Iizuka, Kazuma Sasaki, and Hiroshi Ishikawa. 2016. Learning to simplify: fully convolutional networks for rough sketch cleanup. *ACM Trans. Graph.* 35, 4, Article 121 (July 2016), 11 pages. <https://doi.org/10.1145/2897824.2925972>
- Karan Singh. 2002. A Fresh Perspective. In *Proceedings - Graphics Interface*.
- Tibor Stanko, Mikhail Bessmeltsev, David Bommes, and Adrien Bousseau. 2020. Integer-Grid Sketch Simplification and Vectorization. In *Computer graphics forum*, Vol. 39. Wiley Online Library, 149–161.
- Philip Steadman. 2002. *Vermeer's camera: uncovering the truth behind the masterpieces*. Oxford University Press.
- Ivan E Sutherland. 1964. Sketch pad a man-machine graphical communication system. In *Proceedings of the SHARE design automation workshop*. 6–329.
- Laura M Taylor and Peter Mitchell. 1997. Judgments of apparent shape contaminated by knowledge of reality: Viewing circles obliquely. *British Journal of Psychology* 88, 4 (1997), 653–670.
- Osama Tolba, Julie Dorsey, and Leonard McMillan. 1999. Sketching with projective 2D strokes. In *Proc. UIST* (Asheville, North Carolina, USA). Association for Computing Machinery, New York, NY, USA, 149–157.
- M. Tory and T. Moller. 2004. Human factors in visualization research. *IEEE Transactions on Visualization and Computer Graphics* 10, 1 (2004), 72–84. <https://doi.org/10.1109/TVCG.2004.1260759>
- Dave Pagurek Van Mossel, Chenxi Liu, Nicholas Vining, Mikhail Bessmeltsev, and Alla Sheffer. 2021. StrokeStrip: joint parameterization and fitting of stroke clusters. *ACM Trans. Graph.* 40, 4, Article 50 (July 2021), 18 pages.
- A. Viterbi. 1967. Error bounds for convolutional codes and an asymptotically optimum decoding algorithm. *IEEE Transactions on Information Theory* 13, 2 (1967), 260–269. <https://doi.org/10.1109/TIT.1967.1054010>
- Baoxuan Xu, William Chang, Alla Sheffer, Adrien Bousseau, James McCrae, and Karan Singh. 2014. True2Form: 3D curve networks from 2D sketches via selective regularization. *ACM Trans. Graph.* 33, 4, Article 131 (July 2014), 13 pages.
- Jerry Yin, Chenxi Liu, Rebecca Lin, Nicholas Vining, Helge Rhodin, and Alla Sheffer. 2022. Detecting Viewer-Perceived Intended Vector Sketch Connectivity. *ACM Transactions on Graphics* 41 (2022). Issue 4.
- Byung-Jun Yoon. 2009. Hidden Markov Models and their Applications in Biological Sequence Analysis. *Current genomics* 10 (09 2009), 402–15. <https://doi.org/10.2174/138920209789177575>
- Congyi Zhang, Lei Yang, Nenglu Chen, Nicholas Vining, Alla Sheffer, Francis C.M. Lau, Guoping Wang, and Wenping Wang. 2022. CreatureShop: Interactive 3D Character Modeling and Texturing from a Single Color Drawing. *IEEE Transactions on Visualization and Computer Graphics* (2022), 1–18. <https://doi.org/10.1109/TVCG.2022.3197560>

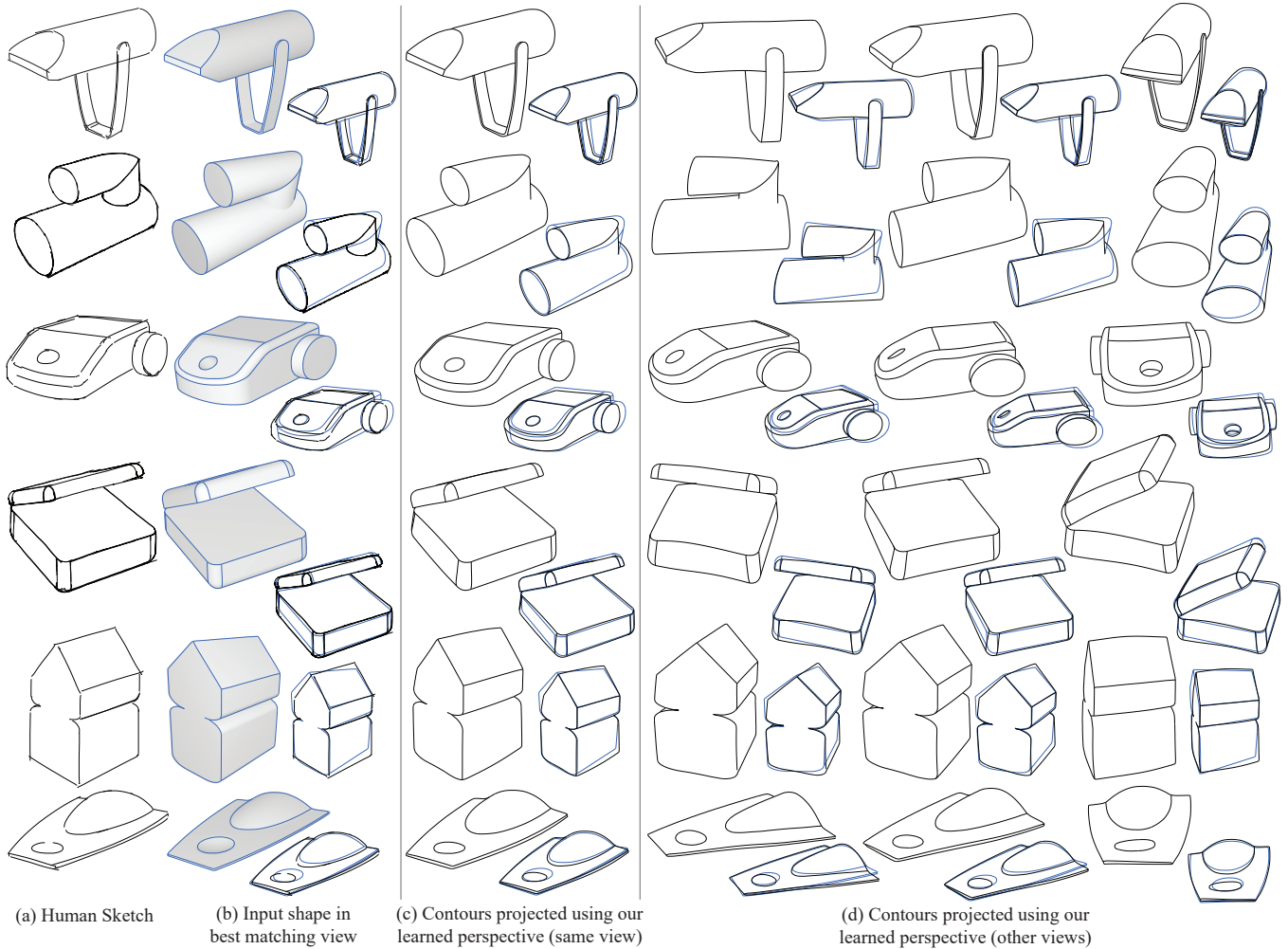


Fig. 5. A gallery of our results. We show (a) human sketch; (b) the input shape and its contours in best matching view (inset overlays the human sketch with contours); (c) our learned output under the same view as (a,b) (inset overlays our output with contours); (d) Applying our learned perspective to contours in different other rotated views (insets overlay our outputs with contours.) In all examples our outputs match the sketch’s perspective deviation.

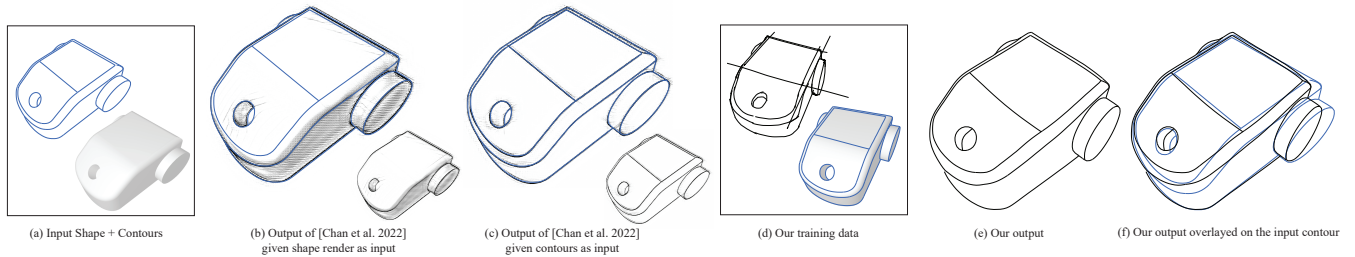


Fig. 6. Comparison. (a) Input shape for [Chan et al. 2022] and ours; (b) output from [Chan et al. 2022] overlaying with the shaded render of the input shape; (c) output from [Chan et al. 2022] overlaying with the input contour; (d) our paired training data; (e) our output overlaying with the shaded render of the input shape; (f) our output overlaying with the input contour. As the examples show, [Chan et al. 2022] faithfully reproduces the analytic perspective in the inputs but does not model human deviations; in contrast, we learn and reproduce the human perspective.

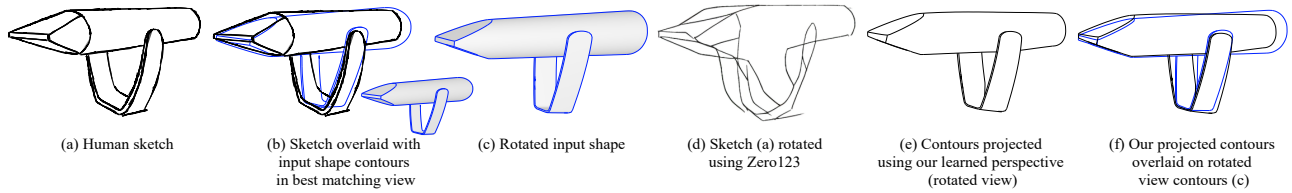


Fig. 7. Comparison versus Zero123 [Liu et al. 2023b], applied to our input human sketch. Left-to-right: (a) input human sketch; (b) 3D projected contours (in blue; inset shows contours overlaid on human sketch); (c) contours in rotated view; (d) Zero123 output for this new view given sketch (a) as input; (e) contours projected using our perspective for the same novel angle. Zero123 introduces degenerate and hallucinated results and fails to preserve object shape. Our rotated view prediction correctly produces a new set of contours that align with viewer expectations and respects the perspective present in the original sketch.

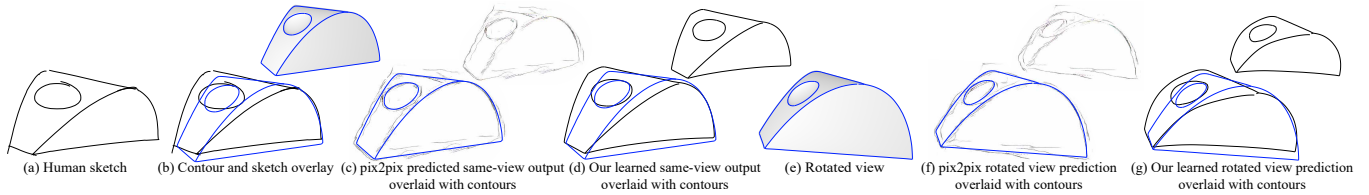


Fig. 8. Comparison to *pix2pix* [Isola et al. 2017], a conditional GAN image-to-image translator, highlights the fact that translation methods are not suited for learning perspective from sparse data. *Pix2pix* trained on our training corpus fails to apply the input human sketch perspective from (a) to the 3D projected contours (b) and introduces spurious lines (c, f); our method correctly learns and applies input sketch perspective to both same- and novel-view contours.

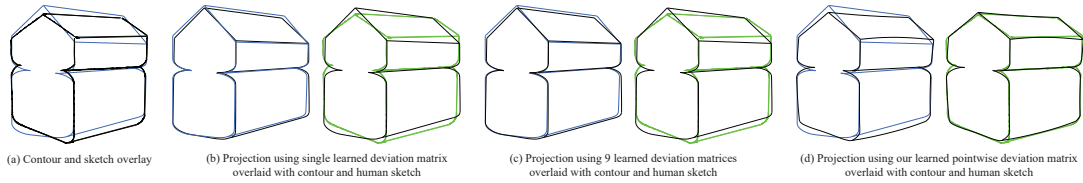


Fig. 9. Ablation. We confirm that capturing human perspective requires a smooth continuous function across object space, by comparing our outputs (d) with those generated using a single deviation matrix per input (b) or using 9 evenly-spaced and interpolated ones (c). Our output (d) reproduces human sketch (a, black) perspective much more faithfully. In each of (b, c, d) overlay of output and contours (blue) on the left, overlay of output and sketch (green) on the right.

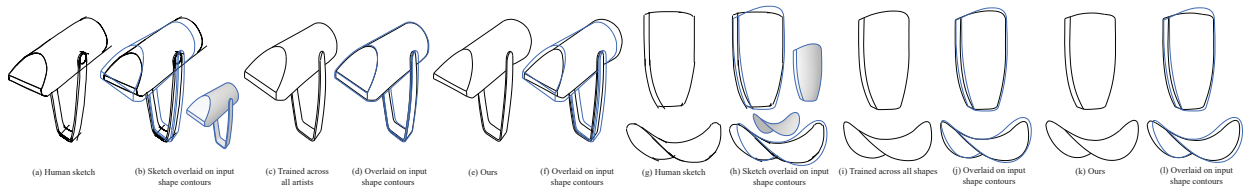


Fig. 10. While we can learn perspective deviation from multiple sketch/object pairs, the results are less expressive than those learned from a single pair. Left: learning from learning from same shape, approximately same view sketches from 6 artists. Right: learning from 10 sketches by the same artist. The latter comes closer to artist perspective, but in all cases our results learned from a single pair are more expressive and better aligned with the training input.

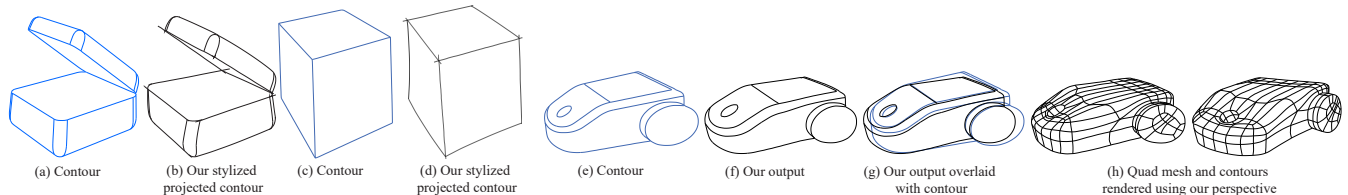


Fig. 11. Applications: (Left) Our perspective can be combined with any stylization method, here we style the contours using [Hähnlein et al. 2022]. (Right) Our perspective learned using contour sketches can be applied as-is to project other surface curves (here, a quad mesh generated by [Nuvoli et al. 2019]).